Direct measurement of pump-induced phase modulation in erbium-doped fibres

Thirstrup, Carsten; Shi, Yuan; Poulsen, Ove; Palsdottir, Bera

Published in:
Proceedings of 5th European Quantum Electronics Conference

Publication date:
1994

Document Version
Publisher's PDF, also known as Version of record

ing spectrum with increasing of the pumping current. Within the limits of the free-running cw generation regime (I_p = 120 mA), no evidence of chirping in the spectrum is observed. The modal chirp appears when passing to the mode-locking regime (I_p = 130 mA), and its value increases with pumping current. As mode-locking develops, the laser spectrum becomes markedly asymmetric (I_p = 150 mA). This effect can be explained by the fact that the dispersion of the laser active medium decreases with wavelength. At I_p = 150 mA, the minimal value of time-bandwidth product $\Delta\tau\Delta v$ = 0.52 was registrated. It should be noted that the optical pulses obtained are not transform-limited ones due to the chirp effect and it is possible to compress them in a medium with a proper dispersion. With further increase in pumping current (I_p = 170 mA), the lasing spectrum broadens (with the corresponding increase in the time-bandwidth product) and becomes symmetric again, which is supposedly due to gain saturation for longer wavelength modes.

An important advantage of the lasers investigated is that their entire spectrum lies in the amplification band of erbium-doped fibers. Being combined with fiber amplifiers, these lasers could serve as a source of soliton pulses with a very high repetition rate. It should be also noted that the measurement of laser characteristics was being carried out during approximately 50 hours of operation under cw pumping and no degradation of spectra or pulse parameters was observed.

CW passive mode-locking was observed for the first time in InGaAsP laser diodes with saturable absorber regions created by the ion implantation. Optical pulses of 650 fs width at 110-GHz repetition rate were obtained in the spectral range of 1.53–1.54 μm. No changes in spectra and autocorrelation traces were observed after 50 hours of cw operation.

Institute of Physics and Technology, Russian Academy of Sciences, 26 Politekhnicheskaya str., St. Petersburg 194021

1. Y. K. Chen, M. C. Wu, T. Tanbun-Ek, R. A. Logan, M. A. Chin, Appl. Phys. Lett. **58**(12), 1253–1255 (1991).
2. K. Y. Lau, IEEE J. of Quant. El. **26**(2), 250–261 (1990).
3. J. H. Zarrabi, E. L. Portnoi, A. V. Chelnokov, Appl. Phys. Lett., 1526–1528 (1991).

Thursday 1st

QThF 1100

Rooms T & U

Special Nonlinear Materials

Jo Zyss, *CNET, France, Presider*

QThF1 1100

Dynamics and origin of the optical Kerr effect in CdSe nanoparticles in the resonant regime

M. Ghanassi, M. C. Schanne-Klein, D. Ricard, C. Flytzanis, *Laboratoire d'Optique Quantique du C.N.R.S., Ecole Polytechnique, 91128 Palaiseau Cedex, France*

In the resonant regime, the optical Kerr effect of CdSe-doped glasses is due to photoexcitation of carriers whose presence modifies the optical properties of the CdSe quantum dots. The recovery time, which governs the repetition rate at which such devices could be operated, is equal to the recombination time of these carriers. At low laser intensity, the recombination time may be shortened by the photodarkening effect.[1] At higher intensity, nonlinear processes such as Auger recombination may play a significant role as aleady suggested[2] although the first data could not clearly make the difference between a cubic (Auger) process or a quadratic one.

Using three different time-resolved techniques, optical phase conjugation, nonlinear absorption, and time-resolved luminescence, we clearly observed that, for a fresh sample, at high laser intensity and for not too long delay times, carrier recombination is dominated by Auger processes. All these data lead to an Auger constant on the order of a few 10^{-30} cm^6 s^{-1}. When the sample has been photodarkened, both the linear nonradiative decay and the Auger process are important.

Understanding the origin of the nonlinearity in these media is also of importance since such artificial materials can, in principle, be tailored to meet specific requirements. The optical Kerr effect may be due to free carriers in which case it corresponds to saturation of the first electronic transition and to induced absorption between the corresponding one-pair state and two-pair states. Alternatively, the photoexcited carriers may be trapped at the surface of the nanoparticles and, through the static electric field they create for example, they may also modify the optical properties.

Time resolving the nonlinear response at low laser intensity and in the degenerate case for samples having experienced various degrees of photodarkening, we have been able to access the relevant mechanisms. Usually, the response shows both a fast component due to free carriers and a slow one due to trapped carriers. The larger the darkening dose is, the smaller the time constant of the fast component and the smaller the magnitude of the slow component. The dominant mechanism is thus observed to depend on the origin of the sample and on its past history. Time-resolving the nonlinear response is the most reliable technique of determining it.

1. P. Roussignol, D. Ricard, J. Lukasik, C. Flytzanis, J. Opt. Soc. Am. B **4**, 5 (1987).
2. P. Roussignol, M. Kull, D. Ricard, F. de Rougemont, R. Frey, C. Flytzanis, Appl. Phys. Lett. **51**, 1882 (1987) and **54**, 1705 (1989).

QThF2 1115

Direct measurement of pump-induced phase modulation in erbium-doped fibres

Carsten Thirstrup, Yuan Shi, Ove Poulsen, Bera Pálsdóttir,* *Mikroelektronik Centret, Technical University of Denmark, Building 345E, 2800 Lyngby, Denmark*

A system, which is able to determine pump induced phase modulation in Er-doped fibres for phase shifts ϕ_p ranging from ~ $\pi/20$ to several π, has been developed. The system (see Fig. 1) consists of a Mach–Zehnder interferometer using a polarization maintaining 3-dB fibre coupler. One arm of the interferometer includes an Er-doped fibre pumped by a 980-nm Ti:sapphire laser. Light from a tunable semiconductor signal laser (λ_s = 1.5 μm–1.6 μm) is coupled to both interferometric arms. A differential detection scheme improves the sensitivity and eliminates influence of amplified spontaneous emission. The phase in the reference arm is linearly modulated in time, $\phi_m = \omega t$, by means of a piezo-electric crystal. This results in a response of the detected signal, which in the case of no pump power can be written;

$$\Delta I_{det} \propto \cos(\omega t + \phi_0),$$

and in presence of pump power;

$$\Delta I_{det} \propto \cos(\omega t + \phi_0 + \phi_p),$$

where ϕ_0 is an arbitrary phase and ϕ_p is the pump-induced phase shift of the signal. ϕ_p is determined by measuring the phase difference of the cosine waveforms before and after the pump is turned on by an optical chopper.

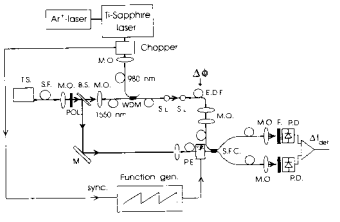

QThF2 Fig. 1. Schematic of the setup for directly measuring pump-induced phase modulation in Er-doped fibres. T.S.: tunable semiconductor laser; S.F.: single mode fibre; M.O.: microscope objective; POL.: polarizer; B.S.: beam splitter; M.: mirror; WDM: 980 nm/1550 nm wavelength demultiplexer; S.L.: spherical lens; E.D.F.: Er-doped fibre; P.E.: piezo-electric crystal; S.F.C.: (polarization maintaining) 3-dB single mode fibre coupler; F.: pump block filter; P.D.: photodiode.

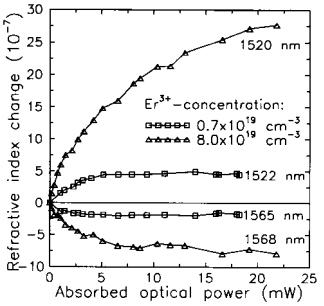

QThF2 Fig. 2. Refractive index change as function of wavelength for Er-doped fibres with a doping concentration of 0.7×10^{19} cm^{-3} (square symbols), 2×10^{19} cm^{-3} (cross symbols), and 8×10^{19} cm^{-3} (triangular symbols). The pump power at 980 nm is 4 mW.

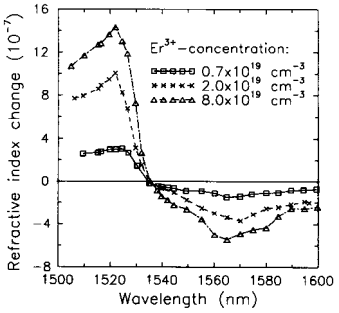

QThF2 Fig. 3. Refractive index change as function of absorbed pump power for Er-doped fibers with doping concentrations of 0.7×10^{19} cm^{-3} (square symbols) and 8×10^{19} cm^{-3} (triangular symbols) at different wavelengths as indicated.

In Fig. 2, the change in refractive index defined as, $\Delta n = (\lambda_s/(2\pi L)\phi_p$, where L is the length of the fibre, is plotted for three fibres with Er^{3+}-doping concentrations of 0.7×10^{19} cm^{-3} (square symbols), 2×10^{19} cm^{-3} (cross symbol) and 8×10^{19} cm^{-3} (triangular symbols) as function of wavelength at an absorbed pump power of 4 mW. The Δn increases with increasing doping concentration and changes sign at λ_s = 1535 nm, which is situated just below a resonance wavelength of 1530 nm. The slope of the curves and therefore the dispersion are maximum near resonance. The dispersion for the fibre with the highest doping concentration is calculated to be ~200 ps/nm/km at 1530 nm.

Figure 3 shows Δn as function of absorbed pump power for the fibres with Er^{3+}-concentrations of 0.7×10^{19} cm^{-3} (square symbols) and 8×10^{19} cm^{-3} (triangular symbols). The wavelengths depicted in Fig. 3, λ_s = 1565 nm and 1568 nm are situated below resonance and the wavelengths λ_s = 1522 nm and 1520 nm are situated above resonance, where a larger Δn can be obtained. The Δn saturates at higher pump powers for the fibre with the higher doping concentration. Thermal effects are believed to be negligible, since a thermal contribution to Δn should be either positive or negative and independent of wavelength, in contrary to the results shown in Fig. 3.

The proposed system has proven to be useful to measure pump-induced phase shifts directly and refractive index changes in Er-doped fibres. The results show that a highly doped fibre should be used if refractive index modulation is desirable (e.g., in optical switches). In applications where the dispersion is unwanted (e.g., in soliton transmission systems), a tradeoff between gain and refractive index modulation should be made for the operating wavelength.

Lycom A/S, NKT Allé 75, 2605 Brøndby, Denmark

QThF3 (Invited) 1130

Two-photon absorption of semiconductor crystallites in doped glasses

G. P. Banfi, V. Degiorgio, M. Ghigliazza, H. M. Tan,* A. Tomaselli, *Dipartimiento di Elettronica, Universitá di Pavia, Via Abbiategrasso 209, Pavia, Italy*

One of the questions concerning semiconductor doped glasses (SDG) is whether the nonlinearities of the crystallites at frequencies well below bandgap are affected by the electronic confinement. The problem has both conceptual and practical implications. Large effects even for modest confinement have been suggested by theoretical models, but the data so far reported are not conclusive to this regard.[1-2] We here report the first quantitative determination of $Im\chi_m^{(3)}$, the imaginary part of the third order susceptibility of the crystallites in SDG. The ten samples investigated are commercial SDG manufactured by Schott, and contain CdTe (RG850-RG830) or CdSSe (CG-495 to RG 715) crystallites.

In order to obtain $Im\chi_m^{(3)}$, one first derives, through a nonlinear transmission measurement, β_{SDG}, the two-photon absorption (TPA) coefficient of the SDG (β_{SDG} is related to $Im\chi_{SDG}^{(3)}$ through $\beta = (\omega(\epsilon_0 c^2 n^2)^{-1} Im\chi^{(3)}$) and then makes use of the relation $\chi_m^{(3)} = \chi_{SDG}^{(3)} f^4 f_v$ with f the local field correction factor, and f_v the volume fraction occupied by the crystallites.[3] The crucial quantities in the procedure are β_{SDG} and f_v.

Since the volume fraction cannot be obtained neither from a wet analysis, nor from the initial composition of the SDG melt, this problem was solved by using small angle neuron scattering measurements (performed at the Cold Neutron facility at NIST, Gaithersburg, Maryland) which provided accurate values of f_v and of the average radius R of the crystallites for each sample.[4] For our samples, f_v = 1.5 − 5%, R = 2-11 nm.

Some transmission data are shown in Fig. 1. In order to obtain a reliable β_{SDG} from an otherwise simple transmission measurement one should take into account the effect of collisional absorption. In fact, the optical pulse is attenuated not only by TPA, but also by the carriers excited by TPA. In the measurements at 1.06 μm (were we employed 30 ps pulses), we could account for collisional absorption, at least for three glasses, by comparing results obtained with samples of different thickness. Another possibility is to employ much shorter pulses, which generate a small number of free carriers. Measurement were done at LENS, Florence, with 200 fs pulses at λ = 0.6 μm. The available wavelength allowed only the study of OG 495, 570, 590.

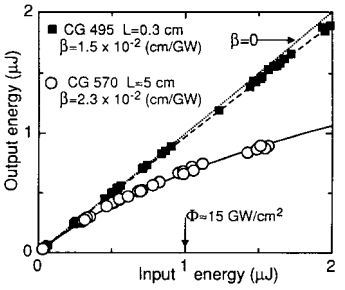

QThF3 Fig. 1. Output energy versus input energy and best fit (solid curves). Femtosecond data at 605 nm.

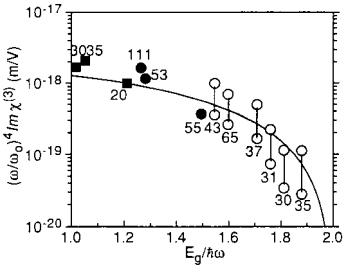

QThF3 Fig. 2. Plot of the scaled quantity $(\omega/\omega_0)^4 Im\chi^{(3)}$ versus $E_g(\hbar\omega)$. Optical measurements at: 0.6 μm (squares), 1.06 μm (circles). The uncertainty for glasses with $E_g/(\hbar\omega)$ > stems from the indeterminacy in collision absorption: the two open circles encompass the possible extreme values. The numbers associated to the experimental points are the radii of the nanocrystals in angstroms. The solid line gives $(\omega/\omega;'i0)^4 Im\chi^{(3)}$ for bulk semiconductors.

The results can be seen in Fig. 2 where we plotted the scaled quantity $(\omega/\omega_0)^4 Im\chi^{(3)}$, with ω_0 the frequency of 1.06 μm radiation, as a function of $Eg(\hbar\omega)$, with E_g the energy gap and $\hbar\omega$ the photon energy. The solid line gives the theoretical value of $(\omega/\omega_0)^4 Im\chi^{(3)}$ for a bulk semiconductor, and, as indicated by Van Stryland,[5] is in agreement with bulk data. $Im\chi_m^{(3)}$ must be quite small, if we note that deviations from the bulk values are not evident even for the small crystallites of the GG 495 glass (R = 2 nm). We can conclude that semiconductor nanocrystals with a size ranging between 2 and 11 nm, the TPA coefficient is comparable to that the bulk semiconductor in the whole accessible range of $E_g/(\hbar\omega)$ values. Such a result calls for a reconsideration of the